



Research Paper

The Impact of Hydrostatic Pressure on Thermal Conductivity of Nanostructured Bi

Tahseen A. HUSAIN¹, Ibrahim Nazem QADER^{1,a}

¹Department of Physics, College of Science, University of Raparin, Rania, Sulaymaneyah, Iraq
^ainqader@gmail.com

Received: 31.05.2022

Accepted: 14.03.2023

Abstract: In this study, a simulation of the theoretical calculation of Lattice thermal conductivity of Bismuth bulk and nanowires with diameters of 98, 115, and 327 nm in the temperature range of 10 – 300 K and pressure range of 0 – 1.6 GPa was investigated. The theoretical approach was compared with experimental data obtained from the literature with the same diameters. These calculations were achieved by using the Morelli Callaway model and the Clapeyron equation that both longitudinal and transverse modes are taken into account. Melting temperature, mass density, unit cell volume, mean bond length, lattice parameter, group velocity and longitudinal and transverse Debye temperature for all transverse and longitudinal modes were calculated for each NW diameter mentioned. Controlling heat transfer by changing mechanical pressure can be an important achievement in practice. The results of this study show that pressure causes different changes in the amount of heat transfer at different temperatures, so that as pressure increases, the amount of heat transfer decreases.

Keywords: Callaway model, Lattice thermal conductivity, Hydrostatic Pressure, Bismuth, Nanowires

1. Introduction

Since the beginning of the new century, electronics have hugely influenced technological development. As Moore's law states, roughly every two years the number of transistors on a microchip doubles. This law has been valid for the last 50 years and it appears to be still valid for the next few years. With the ongoing reduction of feature sizes, the components of a microchip can be scaled down without changes in their performance [1]. Nanowires (NWs) have many current and prospective applications in electronics, they can be made using different techniques using metals, semimetal, or semiconductors. The lattice thermal conductivity (LTC) (κ_L or κ for simplicity) refers to the ability of the heat transfer through a sample that has a temperature difference at both ends, which is considered to be one of the most important thermoelectric parameters in determining the efficiency of energy conversion of thermoelectric materials. Due to the importance, in most energy techniques, lattice thermal conductivity (LTC) of crystalline materials is having great interest in academic and industrial research [2]. The theoretical approach in the calculation of (LTC) for different kinds of materials is very important for science and technology. It would help in understanding the dissipation of heat in microelectronic and nanoelectronics [3]. Modified Callaway's theory can be used to calculate lattice thermal conductivity (LTC) for different kinds of nanowires such as Bismuth nanowire.

Bismuth, which is a semimetal, has unique electronic properties because of its low density, the small effective mass ($m_{eff} \approx 10^{-3}m_e$, where m_e is the free electron mass) and the long mean free path of the carriers (about 2 μm at 300 K and up to 1 mm at 4.2 K), high de Broglie wavelength, strongly anisotropic and small Fermi surface. These properties are of high interest for future applications of electronic quantum confinement effects in low-dimensional bismuth structures [4]. It also has a relatively easy ability to fabricate. Bismuth nanostructures have a very wide interest as applications

How to cite this article

Husain T.A., Qader, I. N., "The Impact of Hydrostatic Pressure on Thermal Conductivity of Nanostructured Bi", *El-Cezeri Journal of Science and Engineering*, Vol. 10, No. 2, 2023, pp. 208-221.

ORCID: ^a0000-0003-1167-3799; ^b0000-0003-4008-7019

in electronics/optoelectronics, biomedical, energy storage and conversion, and thermoelectric [5]. Bismuth nanowires of less than 100 nm diameter have attracted much attention in theoretical and experimental studies because of their small electron-effective mass that allows the study of quantum confinement effects at a diameter of (~ 40 nm). However, few direct measurements of Bismuth thermal conductivity have been made, which has a significant interplay between electrons, holes, and phonons as heat carriers [6]. In Bismuth, thermal conductance is mainly achieved by the electronic contribution from 100 to 300 K, while thermal conductance below 50 K is mainly achieved by phonons [7]. Also, the thermoelectric properties of Bismuth nanowires show improvements compared to the bulk material. Superconductivity has been observed for a Bismuth nanowire with a diameter of 72 nm with a clear Shubnikov de Haas effect below the superconducting transition temperature [8].

The efficiency of thermoelectric devices based on the thermoelectric figure of merit (ZT) value of a given material, defined as $ZT = S^2\sigma T/\kappa$. Single-crystalline Bismuth nanowires have been of great importance due to the expected quantum confinement effect, which should enhance the power factor without significantly affecting κ [9].

In this paper we adopted a simulation which is based on a modified Callaway model to calculate the LTC of Bismuth for bulk and nanowires with diameters of (98, 115, and 327 nm) at pressures of up to 1.8 GPa. The results were compared with experimental data, which can be found in the literature [9].

2. Theory and Calculations

A useful way to calculate the lattice thermal conductivity is to use the Debye-Callaway model within the relaxation time approach, The relaxation time in the model can be written as a function of the Debye temperature (θ), the phonon velocity (v) and the Grüneisen parameter (γ).

The lattice thermal conductivity of a material is given by a mathematical model developed by Callaway [10] based on the Boltzmann distribution which is composed of two terms:

$$\kappa = \kappa_1 + \kappa_2 \quad (1)$$

$$\kappa_1 = \frac{1}{3}AT^3 \int_0^{\theta/T} \frac{\tau_c x^4 e^x}{(e^x - 1)^2} dx, \quad (2)$$

$$\kappa_2 = \frac{1}{3}AT^3 \frac{\left[\int_0^{\theta/T} \frac{\tau_c x^4 e^x}{\tau_N (e^x - 1)^2} dx \right]^2}{\left[\int_0^{\theta/T} \frac{\tau_c x^4 e^x}{\tau_N \tau_R (e^x - 1)^2} dx \right]} \quad (3)$$

where

$$A = \frac{k_B^4}{2\pi^2 \hbar^3 v} \quad (4)$$

$$x = \frac{\hbar\omega}{k_B T} \quad (5)$$

where k_B , \hbar , θ , v , T and ω are the Boltzmann constant is 1.38×10^{-23} m²kg/sK, the Plank reduced constant equal to 1.05×10^{-23} Js, the Debye temperature, the acoustic group velocity, the absolute temperature, and the phonon frequency, respectively.

In these equations, τ_R is the scattering time due to resistive processes, τ_N is the scattering time due to normal phonon processes, and $\tau_c^{-1} = \tau_R^{-1} + \tau_N^{-1}$ is the combined scattering rate [11, 12]. κ depends

on the total phonon relaxation time τ_c and the temperature of the material at which the sample is being measured.

There are different processes that scatter phonons are assumed to be independent of each other and to be denoted by individual scattering rates τ_i^{-1} [13]:

$$\tau_c^{-1} = \sum_i \tau_i^{-1} \tag{6}$$

$$\tau_c^{-1} = a\omega^4 + bT^3\omega^2e^{-\theta/T} + \frac{v}{L} \tag{7}$$

where $a\omega^4$ represents the isotope scattering, $bT^3\omega^2e^{-\theta_D/T}$ is the Umklapp process, and $\left(\frac{v}{L}\right)$ is boundary scattering, and a and b are constants [14].

The development of the Callaway model was proposed by Asen-Palmer et al. [15]. He successfully modelled the LTC for Ge based on three acoustic modes, where κ is written as a sum of one longitudinal (κ_L) and two transverse (κ_T) acoustic phonon branches [16, 17],

$$\kappa = \kappa_L + \kappa_{T_1} + \kappa_{T_2} \tag{8}$$

where

$$\kappa_L = \kappa_{L_1} + \kappa_{L_2} \tag{9a}$$

$$\kappa_T = \kappa_{T_1} + \kappa_{T_2} \tag{9b}$$

κ_{L_1} and κ_{L_2} are the usual Debye-Callaway terms given by [18]:

$$\kappa_{L_1} = \frac{1}{3}A_L T^3 \int_0^{\theta_L/T} \frac{\tau_c^L x^4 e^x}{(e^x - 1)^2} dx, \tag{10}$$

$$\kappa_{L_2} = \frac{1}{3}A_L T^3 \frac{\left[\int_0^{\theta_L/T} \frac{\tau_c^L x^4 e^x}{\tau_N^L (e^x - 1)^2} dx \right]^2}{\int_0^{\theta_L/T} \frac{\tau_c^L x^4 e^x}{\tau_N^L \tau_R^L (e^x - 1)^2} dx} \tag{11}$$

and similarly, for the transverse phonons [19],

$$\kappa_{T_1} = \frac{1}{3}A_T T^3 \int_0^{\theta_T/T} \frac{\tau_c^T x^4 e^x}{(e^x - 1)^2} dx, \tag{12}$$

$$\kappa_{T_2} = \frac{1}{3}A_T T^3 \frac{\left[\int_0^{\theta_T/T} \frac{\tau_c^T x^4 e^x}{\tau_N^T (e^x - 1)^2} dx \right]^2}{\int_0^{\theta_T/T} \frac{\tau_c^T x^4 e^x}{\tau_N^T \tau_R^T (e^x - 1)^2} dx}, \tag{13}$$

$$A_L = \frac{k_B^4}{2\pi^2 \hbar^3 v_L}, \tag{14a}$$

$$A_T = \frac{k_B^4}{2\pi^2 \hbar^3 v_T}, \tag{14b}$$

L and T are the longitudinal and transverse phonons, respectively, and θ_L and θ_T are Debye temperatures for the longitudinal and transverse phonon branches, respectively, which represent the temperature of crystal's highest mode of vibration.

The value of Debye temperature can be obtained by using [20]:

$$\theta_{L(T)} = \left(\frac{\omega_{L(T)} \pi^2}{V} \right)^{1/3} \frac{\hbar v_{L(T)}}{k_B}, \quad (15)$$

where V is the volume per atom and $\omega_{L(T)}$ longitudinal (transverse) phonon frequency. This equation can be applied when there is no pressure.

Another important factor that effects lattice thermal conductivity is the relation between melting temperature and pressure. Melting temperature $T_m(P)$ of stable bulk Si in the diamond structure decreases as the pressure P increases, or $dT_m/dP < 0$ [21].

The classic Clapeyron equation may be useful to obtain the T–P curve theoretically in the following relation [22]:

$$dP = \frac{H_m(T_m, P)}{\Delta V_m(T_m, P) T_m} dT_m \quad (16)$$

where $H_m(T_m, P)$ and $\Delta V_m(T_m, P) T_m$ are the molar melting enthalpy and the molar volume change during melting respectively.

In order to solve the Clapeyron equation we may assume a first-order approximation as $H_m(T_m, P) \approx H_m(T_m)$ and $\Delta V_m(T_m, P) \approx \Delta V_m(P)$ which simplifies equation (16) to

$$dP = \frac{H_m(T_m)}{\Delta V_m(P) T_m} dT_m \quad (17)$$

In equation (17) the $H_m(T_m)$ function can be obtained from the Helmholtz function [23]:

$$H_m(T_m) = G_m(T_m) - T_m dG_m(T_m)/dT_m, \quad (18)$$

where $G_m(T_m)$ is the temperature dependent solid–liquid Gibbs free energy difference.

$$G_m(T_m) = H_{m0} T_m (T_{m0} - T_m) / T_{m0}^2 \quad (19)$$

where T_{m0} is the melting temperature at $P = 0$, for bulk state T_{m0} equal to T_∞ while NW with a diameters (r) represented by $T_m(r)$, and H_{m0} is the bulk molar melting enthalpy at T_{m0} .

$$H_m T_m = H_{m0} (T_m / T_{m0})^2 \quad (20)$$

In equation (17),

$$\Delta V_m(P) = (V_l - V_s) + (\Delta V_l - \Delta V_s), \quad (21)$$

V_s is the molar volume of the crystal and V_l is the molar volume in the liquid state.

$$\Delta V_l = -V_l P_l K_l \quad \text{and} \quad \Delta V_s = -V_s P_s K_s$$

To find a solution of equation (21), a relationship between two pressures of P_l and P_s must be found. Therefore, we consider aspherical particle with a diameter D , then the Laplace–Young equation, $P_s = 4f/D$ and $P_l = 4\gamma/D$ for the particle in a solid state and in a liquid state, respectively, where γ is the surface energy and f is stress [24]. Then $P_s/P_l = f/\gamma$, substituting this relationship into $\Delta Vm(P)$:

$$\Delta Vm(P) = V_l - V_s + [V_s K_s - V_l(\gamma/f)K_l]P \tag{22}$$

Integrating equation (16) from 0 to P and T_m from T_{m0} to T_m in terms of equations (19) and (22),

$$\int_0^P \left\{ V_l - V_s + \left[V_s K_s - V_l \left(\frac{\gamma}{f} \right) K_l \right] P \right\} dP = (H_{m0} T_{m0}^2) \int_{T_{m0}}^{T_m} T_m dT_m$$

yields

$$T_m(P) = T_{m0} \sqrt{1 + \frac{\{2(V_l - V_s)P + [V_s K_s - V_l(\gamma/f)K_l]P^2\}}{H_{m0}}} \tag{23}$$

In equation (22), γ is the surface energy, and f is the surface stress. $\gamma \neq f$ for solid, and $\gamma = f$ in liquids [24]. The surface stress of liquid and solid is represented by (f_{sl}) for bulk is:

$$f_{sl}(\infty) = (h/2)[3S_{vib}(\infty)H_{m0}(\infty)/K_s V_s R]^{1/2} \tag{24}$$

where h is height of the first solid surface layer, S_{vib} is the vibrational component of melting entropy, and R is the ideal gas constant.

For NWs

$$f_{sl}(r) = (h/2)[3S_{vib}(r)H_{m0}(r)/K_s V_s R]^{1/2} \tag{25}$$

The rate of surface energy γ_{sl} for bulk is,

$$\gamma_{sl} = 2hS_{vib}(\infty)H_m(\infty)/(3V_s R) \tag{26}$$

And for NWs

$$\gamma_{sl} = 2hS_{vib}(r)H_m(r)/(3V_s R) \tag{27}$$

where S_{vib} is the vibrational part of the overall melting entropy.

For bulk crystal, the mean bond length which is written as $d_{mean}(\infty)$ is constant and for nanoscale range denoted by $d_{mean}(r)$ its size increases with the decrease of r , and when the value of r approaches $3h$ the mean bond length reaches a critical and its maximum value which is denoted by $d_{mean}(r_c)$. The change of mean bond length is as follows;

$$\Delta d_{mean}(r) = \Delta d_{mean}(r_c) \left[\exp \left(\frac{-2(S_m(\infty) - R)}{3R \left(\frac{r}{r_c} - 1 \right)} \right) \right]^{1/2} \tag{28}$$

R is the ideal gas constant and ($r_c = [3 - D]h$), where D might be 0, 1, or 2 for quantum dots, NW, and nanolayer, respectively, and h and $d_{mean}(r)$ can be obtain from, $h = 1.429 d_{mean}(\infty)$ [25]. S_m is the overall melting entropy and is expressed as follows [26]:

$$S_m(\infty) = H_m(\infty)/T_m \quad (29)$$

where $H_m(\infty)$ is the melting enthalpy, and is found as follows:

$$H_m(\infty) = -10^{-5} T_m^2(\infty) + 0.059 T_m(\infty) - 21.33 \quad (30)$$

$H_m(\infty) = 26.37 \text{ J}\cdot\text{mol}^{-1}$ [25], T_m is in K, H_m is in J/ mole.

The bulk melting entropy is given by:

$$S_m(\infty) = S_{vib}(\infty) + R \quad (31)$$

The mean bond length is calculated using the equation below [25].

$$d_{mean}(r) = h - \Delta d_{mean}(r) \quad (32)$$

and the bulk mean bond length is,

$$d_{mean}(\infty) = h - \Delta d_{mean}(r_c) \quad (33)$$

The size-dependent lattice constant ($a(r)$) in nanoscale at free pressure ($P = 0$)

$$a(r) = \frac{4}{\sqrt{3}} d_{mean}(r) \quad (34)$$

Then the size-dependent lattice volume ($V(r)$) at free pressure is determined from the following equation

$$V(r) = \left[\frac{a(r)}{2} \right]^3 \quad (35)$$

The mass density $\rho(r)$ of nanocrystalline materials is given by [27],

$$\rho(r) = \rho(\infty) \frac{V(\infty)}{V(r)} \quad (36)$$

$\rho(\infty)$ is the bulk material's mass density, and $V(\infty)$ is the volume unit cell in the bulk state. The bulk density of crystals $\rho(\infty)$ is given by [28]:

$$\rho(\infty) = \frac{M}{N_A V(\infty)} \quad (37)$$

The average molar mass of Bismuth which is used in this equation ($M = 41. \cdot 10^{-26} \text{ kg}$). At room temperature and zero pressure the bulk modulus $B(\infty)$ is related to bulk group velocity v_g as follows [29]:

$$B(\infty) = v_g^2(\infty) \rho(\infty) \tag{38}$$

To compute the nanoscale bulk modulus we use;

$$B(r) = v_g^2(r) \rho(r) \tag{39}$$

The group velocity v_g in equation (39) includes acoustic and optical phonons, and each one of them has one longitudinal and two transverse polarisation branches. Thus, the mean group velocity is determined as follows,

$$\frac{1}{v_g^{Total}} = \frac{1}{v_g^L} + \frac{2}{v_g^T} \tag{40}$$

The relation between the group velocity and the Debye temperature for isotropic system zero pressure, can be expressed as [30];

$$V_g(r) = V_g(\infty) \frac{\theta_D(r)}{\theta_D(\infty)} \tag{41}$$

where $\theta_D(r)$ is the size-dependent Debye temperature, and $\theta_D(\infty)$ is the bulk Debye temperature. The Debye temperature of the nanowire (NW) can be determined as follows.

$$\theta_D(r) = \theta_D(\infty) \left[\frac{T_m(r)}{T_m(\infty)} \right]^{1/2} \tag{42}$$

where $T_m(\infty)$ $T_m(r)$ denotes to the bulk and nanosized dependent melting temperatures respectively at (P = 0). $T_m(r)$ can be determined as follows,

$$T_m(r) = T_m(\infty) \left(\frac{V(r)}{V(\infty)} \right)^{2/3} \exp \left(\frac{-2(S_m(\infty)-R)}{3R \left(\frac{r}{r_c} \right) - 1} \right) \tag{43}$$

The parameters of Bismuth that are utilized to measure the LTCs under pressure in bulk and NW have diameters of 50 nm, 63 nm, 66 nm, 100 nm, and 148 nm, as shown in Table 1.

Table 1. Universal constants and some specific parameter for Bismuth

Ideal gas constant	R	8.314 (JK ⁻¹ mol ⁻¹)	Ref. [31]
Avogadro number	N_A	6.02 × 10 ²³	
Melting temperature	T_m	544.5 (K)	
Enthalpy of fusion	H_m	53.146 (J.g ⁻¹)	Ref. [32]
First surface layer height	h	0.4078 (nm)	From Eq. (17)
Bulk overall melting entropy	$S_m(\infty)$	30 (JK ⁻¹ mol ⁻¹)	From Eq. (20)
	S_{vib}	21.686 (JK ⁻¹ mol ⁻¹)	
Mass density	ρ	9800 (kg.m ⁻³)	
Elastic constant	$c11$	63.37 (GPa)	
	$c12$	24.49 (GPa)	
	$c44$	11.57 (GPa)	
Average atomic mass		208.98038 (amu)	Ref. [31]
Weight factor	η	0.55	Ref. [33]
Effective mass	m^*	0.113 m_e	Ref. [31]

Eq. (21) is also applicable for nanocrystals if we substitute T_{mo} in Eq. (21) by size-dependent melting temperature at zero pressure T_{mo}' . The quantitative value of T_{mo}' is determined according to Lindemann's criterion for melting as [34];

$$T_{mo}' = T_{mo} \exp\{-2S_{vib}/3R\} / [(r/r_0) - 1] \quad (44)$$

In Eq. (44) $r_0 = 3h$ where all atoms are located on their surfaces.

$$T_m(P) = T_{mo}' \sqrt{1 + \frac{\{2(V_l - V_s)P + [V_s K_s - V_l(\gamma/f)K_l]P^2\}}{\Delta H_{mo}}} \quad (45)$$

Figure 2 shows the relation of the melting temperature of Bismuth nanocrystal with its size and pressure, and as a result, it is found that the melting temperature of Bismuth nanowires is lower than the melting temperature of bulk. In Eq. (43), V_s represents the molar volume of the crystal, which is defined by [34];

$$V_s(r) = V_l(r)N_A, \quad (46)$$

$$\frac{v_l}{v_s} = 0.9. \quad (47)$$

The compressibility values $K_s(r)$ can be determined by:

$$K_l/K_s = 10. \quad (49)$$

The calculations in the present study were achieved by using the Morelli Callaway model and the Clapeyron equation at pressures ranging from 0 to 1.8 GPa. A list of additional calculated parameters for the Bismuth NWs is presented in Table 2.

Table 2. The estimated size dependence parameters for Bi NWs and bulk

r (nm)	98	115	327	Bulk
d_{mean} (Å)	2.8626	2.8613	2.8564	2.8537
a (Å)	6.6110	6.6079	6.5965	6.5904
V (Å ³)	36.1171	36.0671	35.8814	35.7813
ρ (kg.m ⁻³)	9708	9722	9772	9800
T_m (K)	539.96	540.63	543.14	544.5
θ_D^l (K)	121.17	121.43	122.42	122.96
θ_D^{T1} (K)	62.54	62.62	62.91	63.06
θ_D^{T2} (K)	48.28	48.34	48.57	48.68
v_L (m.s ⁻¹)	2345	2350	2369	2380
v_{T1} (m.s ⁻¹)	1397	1398	1405	1408
v_{T2} (m.s ⁻¹)	1077	1079	1084	1087

Table 3 shows some of the relevant data that used to calculate LTC for Bi nanowires and bulk.

Table 3. The fitting parameters of Bi NWs used in this work for calculating LTC for each diameter r (nm)

	r (nm)			
	98	115	327	Bulk
N_{imp} (m ⁻³)	9.0×10^{25}	8.0×10^{25}	3.0×10^{25}	5.0×10^{21}
N_D (m ⁻²)	6×10^{16}	5×10^{16}	1×10^{16}	9×10^{11}
n_e (m ⁻³)	2.5×10^{25}	2×10^{25}	1.18×10^{25}	3×10^{18}
ε	0.002	0.001	0.0007	
L_c (nm)	98	115	327	
L (μm)	5	5	5	300
γ_L	0.012	0.011	0.009	6
γ_T	0.011	0.010	0.008	0.7

3. Results and Discussion

In this study, the thermal conductivity of Bismuth NW and bulk was calculated as a function of temperature at different pressures ranging from 0 to 1.6 GPa, as shown in Fig. 1.

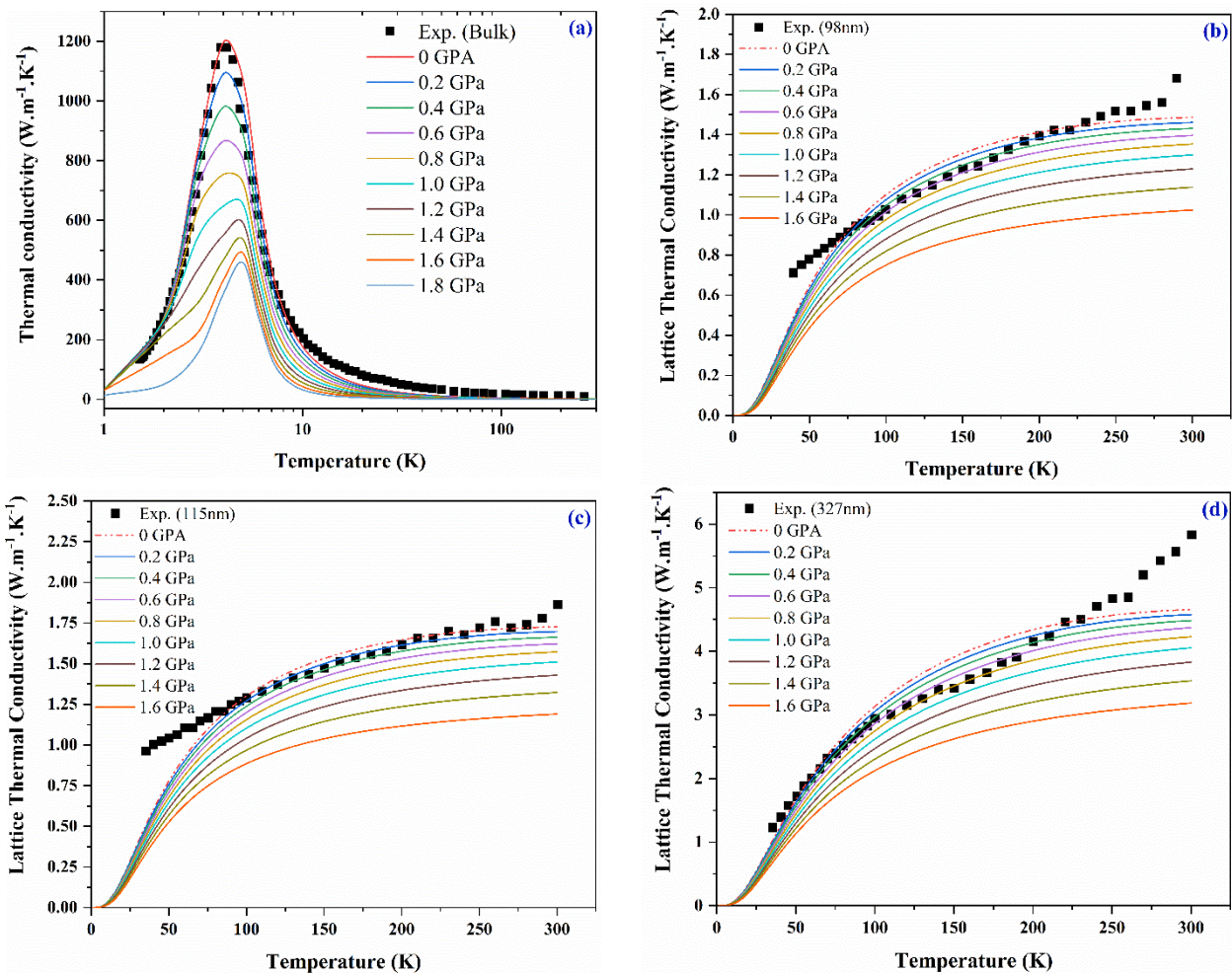


Figure 1. Lattice thermal conductivity of Bi for (a) bulk and (b-d) nanowires as a function of temperature and hydrostatic pressure

Figure 1(a) represents the temperature dependence of LTC for the Bismuth bulk, where the black solid square curve represents the experimental data and the theoretical LTC fits with the experimental data at $P=0$ Pa. From the graph thermal conductivity is very low at $T = 0$ (K) then as the temperature

increases, so the more vibrations resulting in increasing phonon propagation and higher thermal conductivity, which have maximum value at $T = 5 \text{ K}$. Thus, at low temperature both boundary and phonon-electron scattering have significant effects on LTC. Then the curve declines and approach a very low value at $T > 100 \text{ (K)}$. Additionally, the LTC peak shifts to higher temperature by increasing the hydrostatic pressure. Pressure can directly decrease interatomic distance and hence the scattering increases. The other colored lines represent the effect of pressure on the sample which clearly seen that as the pressure increases the thermal conductivity decreases. Figures 1 b-d show the influence of thickness on the conductivity of Bismuth NW with diameter 98, 115 and 327 nm in the temperature range 10 – 300 K and pressure range 0 – 1.6 GPa. In the mentioned graphs the thermal conductivity of Bismuth nanowires increase as the temperature increases however the real temperature-dependent behaviors are different with different diameter at the same pressure. As the diameter decreased the lattice thermal conductivity of Bismuth is decreased, because thermal conductivity depends on many factors, includes the structure of the atomic arrangement. It is known that the periodicity of atoms in the core of nanowire is similar to its bulk material, however from the center to the surface, the interatomic distances increases [35]. It is clearly seen that when going from bulk to nanowire, the bulk thermal conductivity at low temperature is higher than that of nanowire thermal conductivity due to alternate contributions to phonon scattering.

3.1. Melting temperature of Bismuth in Bulk and NW Forms

Figure 2 reveals the melting temperature of Bismuth nanowire as a function of pressure, and thickness. In the graph the relationship of melting temperature with diameter is constant at low pressure, but as the pressure increases and reaches 1.5 GPa melting temperature shows a sharp decline and reaches a very low value. Yang and colleague [36] showed that melting temperature decreases with increasing pressure. They predicted melting temperature as a function of pressure using Clapeyron equation. Their result confirms the experimental data obtained for Ge bulk. However, in the nanoscale dimension, size dependent parameters also affect melting temperature.

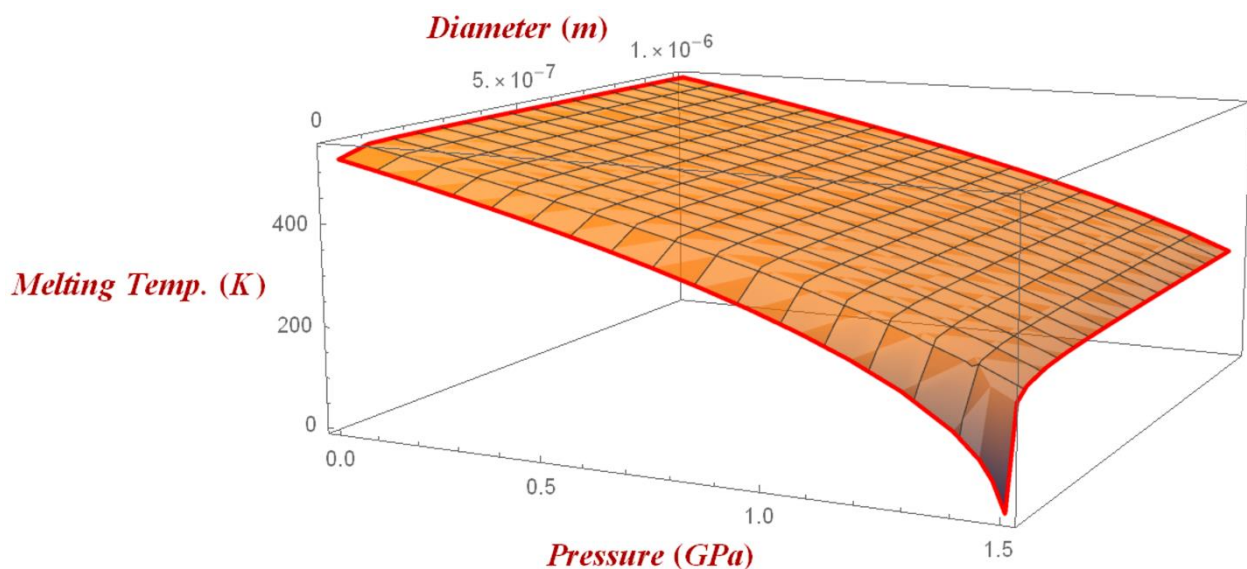


Fig. 2. A 3D plot of melting temperature vs. diameter and pressure

In solid state physics, when pressure is applied on a solid, the lattice thermal conductivity decreases, and heat movement is controlled by phonons, these phonons behave as heat carriers.

3.2. Pressure-dependent Lattice thermal conductivity - of Bismuth

Figure 3a depicts the Lattice thermal conductivity LTC of Bismuth as a function of pressure ranging

from 0 to 1.8 GPa for bulk at different diameters of (98, 115, 327 nm) nanowires at a temperature of 300 K. The graph shows that lattice thermal conductivity decreases as the pressure increases, and that's occurring more clearly with the bulk. Figure 3b shows the lattice thermal conductivity of bulk Bismuth at different temperatures, the thermal conductivity of the Bismuth was estimated theoretically. The minimum value of LTC (P) for bulk Bi is recorded at 300 K and 1.8 GPa which is $0.2 \text{ (W/m}^{-1} \text{ K}^{-1}\text{)}$, and the maximum value obtained at pressure-free LTC is $3 \text{ W/m}^{-1} \text{ K}^{-1}$.

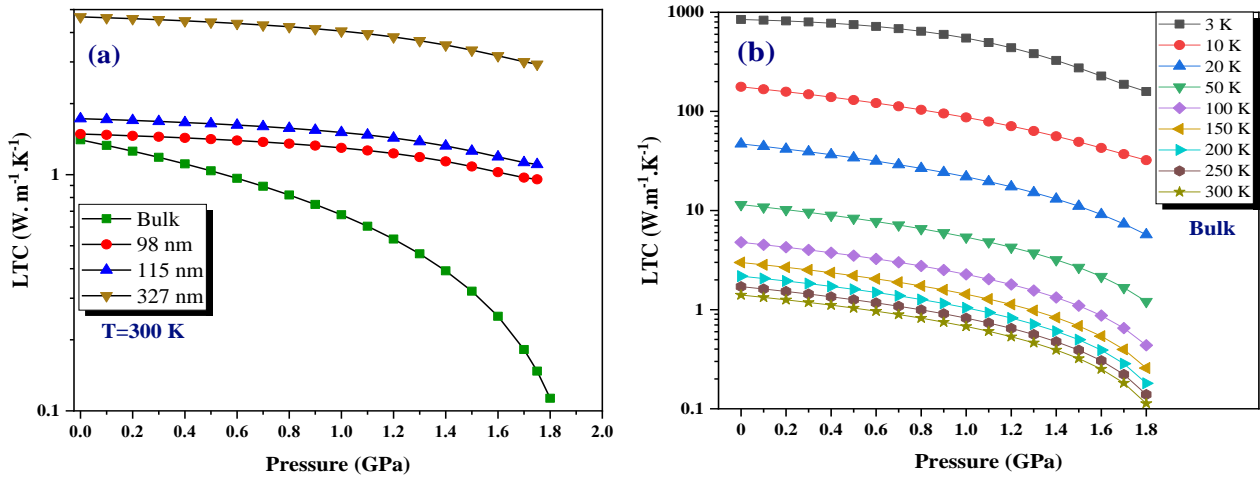


Figure 3. LTC as a function of hydrostatic pressure at (a) room temperature (300 K), (b) temperature from 3 to 300 K

3.3. Density and Bulk Modulus of Bismuth

Figure 4(a) shows the relationship between calculated atomic bond density and diameter, while Fig. 4(b) shows relationship between bulk modulus and diameter. The spacing between Bismuth atoms is the shortest at the lowest density. When the atoms' sizes shrank their density will increase, and hence their diameters will decrease as well, which will affect physical and chemical properties [27].

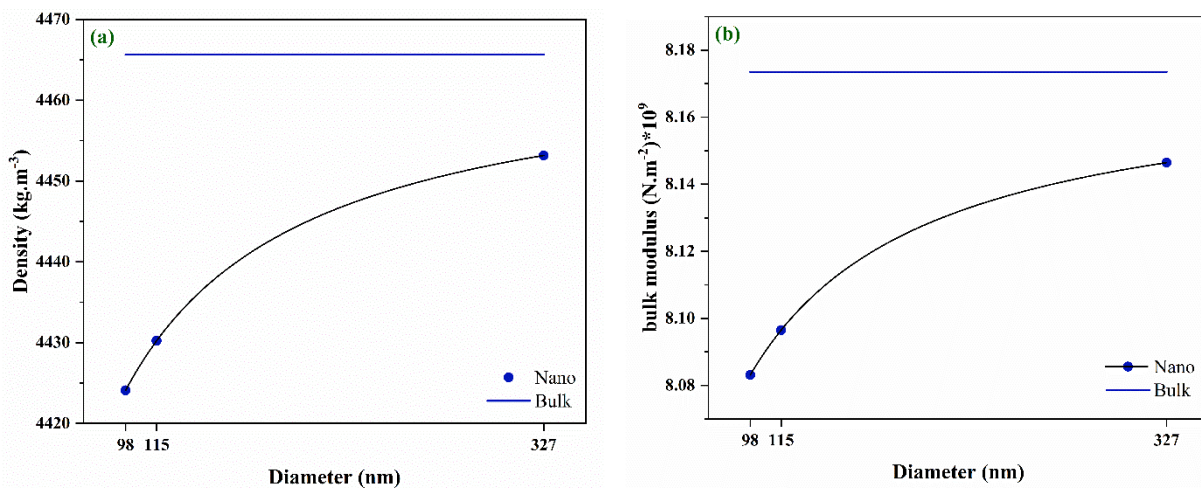


Figure 4. (a) Mass density and (b) bulk modulus for nano and bulk Bi

3.4. Compressibility, Solid Molar Volume, and Liquid Molar Volume of Bismuth

In this section, the compressibility, solid molar volume, and liquid molar volume for both Bismuth NWs and bulk have all been determined. The relationship between diameter and compressibility with diameters of 98, 115, and 327 nm is shown in Fig. 5(a), where the compressibility decreases as the diameters increased.

Figure 6(a) and (b) shows the change of molar volume for solids and liquids as diameters increase. It is clearly seen from the graph that molar volume for both solids and liquids decrease as the diameter increases.

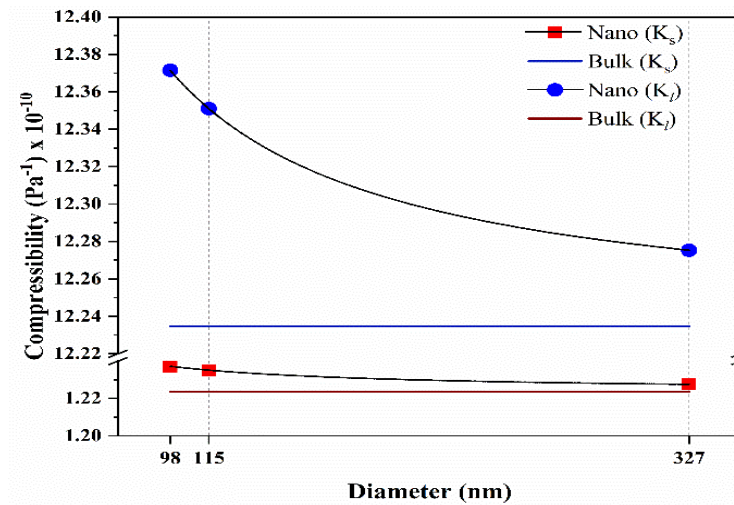


Figure 5. Compressibility for both K_s and K_l for nano and bulk Bi

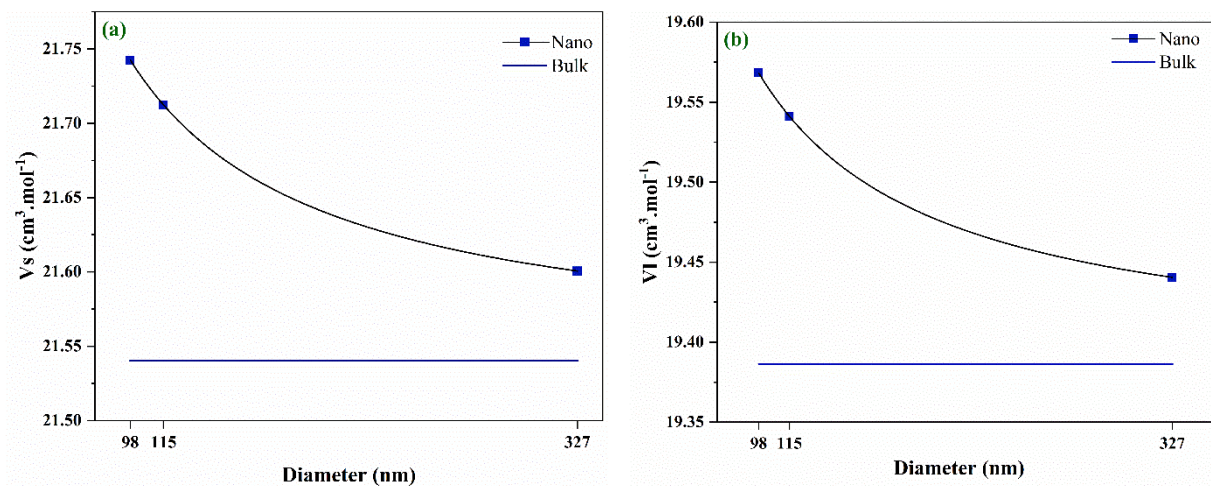


Figure 6. Solid and liquid molar volumes for Bi nano and bulk

4. Conclusions

By using Debye-Callaway model, LTC for Bismuth bulk and nanowires with diameter 98, 115 and 327 nm under pressure range 0 – 1.6 GPa was studied. For the Bismuth bulk the experimental data, and the theoretical calculated data where no pressure exerted fits well. Lattice thermal conductivity decreases as the pressure increases, and that's occur more clearly with bulk. The thermal conductivity of Bismuth nanowires increase as the temperature increases however the real temperature-dependent behaviors are different with different diameter at the same pressure. The bulk thermal conductivity at low temperature is higher than that of nanowire thermal conductivity due to alternate contributions to phonon scattering. On the other hand, the relation of the diameter of Bismuth NW with melting temperature is constant at low pressure, but as the pressure increases and reaches 1.5 GPa melting temperature shows sharp decline and reaches a very low value.

Acknowledgment

The authors would like to thank University of Raparin for its financial support.

Authors' Contributions

INQ coded and obtained all computational parameters. TAH wrote up the article. Both authors read and approved the final manuscript.

Competing Interests

The authors declare that they have no competing interests.

References

- [1]. T. W. Cornelius and M. E. Toimil-Molares, "Finite-and quantum-size effects of bismuth nanowires," *Intech: Rijeka*, Croatia, 2010.
- [2]. S. Nag, A. Saini, R. Singh and R. Kumar, "Ultralow lattice thermal conductivity and anisotropic thermoelectric performance of AA stacked SnSe bilayer," *Applied Surface Science*, vol. 512, 145640, 2020.
- [3]. S. M. Mamand and M. S. Omar, "Effect of Parameters on Lattice Thermal Conductivity in Germanium Nanowires," *Advanced Materials Research*, vol. 832, pp. 33-38, 2014.
- [4]. A. S. Goncharova, K. S. Napolskii, O. V. Skryabina, V. S. Stolyarov, E. E. Levin, S. V. Egorov, A. A. Eliseev, Y. A. Kasumov, V. V. Ryazanov and G. A. Tsirlina, "Bismuth nanowires: electrochemical fabrication, structural features, and transport properties," *Physical Chemistry Chemical Physics*, vol. 22, no. 26, pp. 14953-14964, 2020.
- [5]. K. Liu, C. L. Chien, P. C. Searson and K. Yu-Zhang, "Structural and magneto-transport properties of electrodeposited bismuth nanowires," *Applied Physics Letters*, vol. 73, no. 10, pp. 1436-1438, 1998.
- [6]. H. Goldsmid, "The thermal conductivity of bismuth telluride," *Proceedings of the Physical Society. Section B*, vol. 69, no. 2, pp. 203, 1956.
- [7]. Y.-M. Lin, S. B. Cronin, J. Y. Ying, M. S. Dresselhaus and J. P. Heremans, "Transport properties of Bi nanowire arrays," *Applied Physics Letters*, vol. 76, no. 26, pp. 3944-3946, 2000.
- [8]. M. Tian, J. Wang, Q. Zhang, N. Kumar, T. E. Mallouk and M. H. Chan, "Superconductivity and quantum oscillations in crystalline Bi nanowire," *Nano letters*, vol. 9, no. 9, pp. 3196-3202, 2009.
- [9]. J. W. Roh, K. Hippalgaonkar, J. H. Ham, R. Chen, M. Z. Li, P. Ercius, A. Majumdar, W. Kim and W. Lee, "Observation of Anisotropy in Thermal Conductivity of Individual Single-Crystalline Bismuth Nanowires," *ACS Nano*, vol: 5, no. 5, pp. 3954-3960, 2011.
- [10]. J. Callaway, "Model for lattice thermal conductivity at low temperatures," *Physical Review*, vol. 113, no. 4, pp. 1046, 1959.
- [11]. I. N. Qader and M. S. Omar, "Carrier concentration effect and other structure-related parameters on lattice thermal conductivity of Si nanowires," *Bulletin of Materials Science*, vol. 40, no. 3, pp. 599-607, 2017.
- [12]. I. N. Qader, B. J. Abdullah and M. S. Omar, "Range Determination of the Influence of Carrier Concentration on Lattice Thermal Conductivity for Bulk Si and Nanowires," *Aksaray University Journal of Science and Engineering*, vol. 4, no. 1, pp. 30-42, 2020.
- [13]. D. T. Morelli and G. A. Slack, "High lattice thermal conductivity solids," *High thermal conductivity materials*, Springer, 2006, p. 37-68.
- [14]. G. Joshi, X. Yan, H. Wang, W. Liu, G. Chen and Z. Ren, "Enhancement in thermoelectric figure-of-merit of an N-type half-Heusler compound by the nanocomposite approach," *Advanced Energy Materials*, vol. 1, no. 4, pp. 643-647, 2011.
- [15]. M. Asen-Palmer, K. Bartkowski, E. Gmelin, M. Cardona, A. Zhernov, A. Inyushkin, A. Taldenkov, V. Ozhogin, K. M. Itoh and E. Haller, "Thermal conductivity of germanium crystals with different isotopic compositions," *Physical review B*, vol. 56, no. 15, pp. 9431, 1997.
- [16]. I. N. Qader, H. M. Qadr and P. H. Ali, "Calculation of Lattice Thermal Conductivity for Si Fishbone Nanowire Using Modified Callaway Model," *Semiconductors*, vol. 55, no. 12, pp. 960-967, 2021.

- [17]. I. N. Qader, B. J. Abdullah and H. H. Karim, "Lattice Thermal Conductivity of Wurtzite Bulk and Zinc Blende CdSe Nanowires and Nanoplayer," *Eurasian Journal of Science & Engineering*, vol. 3, no. 1, pp. 9-26, 2017.
- [18]. I. N. Qader, B. J. Abdullah, M. H. Hassan and P. H. Mahmood, "Influence of the Size Reduction on the Thermal Conductivity of Bismuth Nanowires," *Eurasian Journal of Science and Engineering*, vol. 4, no. 3, pp. 55-65, 2019.
- [19]. H. H. Karim, M. S. Omar and I. N. Qader, "Hydrostatic pressure effect on melting temperature and lattice thermal conductivity of bulk and nanowires of indium arsenide," *Physica B: Condensed Matter*, vol. 640, 414045, 2022.
- [20]. D. Morelli, J. Heremans and G. Slack, "Estimation of the isotope effect on the lattice thermal conductivity of group IV and group III-V semiconductors," *Physical review B*, vol. 66, no. 19, 195304, 2002.
- [21]. C. Yang, J. Li and Q. Jiang, "Effect of pressure on melting temperature of silicon determined by Clapeyron equation," *Chemical physics letters*, vol. 372, no. 1-2, pp. 156-159, 2003.
- [22]. L. Q. Lobo and A. G. Ferreira, "Phase equilibria from the exactly integrated Clapeyron equation," *The Journal of Chemical Thermodynamics*, vol. 33, no. 11, pp. 1597-1617, 2001.
- [23]. C. Yang, J. Li and Q. Jiang, "Temperature–pressure phase diagram of silicon determined by Clapeyron equation," *Solid state communications*, vol. 129, no. 7, pp. 437-441, 2004.
- [24]. Q. Jiang, L. Liang and D. Zhao, "Lattice contraction and surface stress of fcc nanocrystals," *The Journal of Physical Chemistry B*, vol. 105, no. 27, pp. 6275-6277, 2001.
- [25]. M. Omar, "Structural and Thermal Properties of Elementary and Binary Tetrahedral Semiconductor Nanoparticles," *International Journal of Thermophysics*, vol. 37, no. 1, pp. 1-11, 2016.
- [26]. I. N. Qader and M. Omar, "Carrier concentration effect and other structure-related parameters on lattice thermal conductivity of Si nanowires," *Bulletin of Materials Science*, vol. 40, no. 3, pp. 599-607, 2017.
- [27]. B. J. Abdullah, Q. Jiang and M. S. Omar, "Effects of size on mass density and its influence on mechanical and thermal properties of ZrO₂ nanoparticles in different structures," *Bulletin of Materials Science*, vol. 39, no. 5, pp. 1295-1302, 2016.
- [28]. J. Stansfeld, "5.7 In Situ Density Measurements," *Measurement of the Thermodynamic Properties of Single Phases*, 208, 2003.
- [29]. B. Abdullah, M. Omar and Q. Jiang, "Size dependence of the bulk modulus of Si nanocrystals," *Sādhanā*, vol. 43, no. 11, pp. 1-5, 2018.
- [30]. M. Hamarashid and M. Omar, "Hydrostatic pressure effects on the processes of lattice thermal conductivity of bulk Silicon and nanowires," *Bulletin of Materials Science*, vol. 44, no. 3, pp. 1-11, 2021.
- [31]. O. Madelung, "Semiconductors: data handbook," *Springer Science & Business Media*, 2012.
- [32]. D. G. Archer, "Enthalpy of Fusion of Bismuth: A Certified Reference Material for Differential Scanning Calorimetry," *Journal of Chemical and Engineering Data*, vol. 49, no. 5, pp. 1364-1367, 2004.
- [33]. C. K. Caylor J, Stuart J, Colpitts T, Venkatasubramanian R, "Enhanced thermoelectric performance in PbTe-based superlattice structures from reduction of lattice thermal conductivity," *Applied physics letters*, 87, 2005.
- [34]. C. Yang and Q. Jiang, editors. Effect of pressure on melting temperature of silicon and germanium. Materials Science Forum, 2005, Trans Tech Publ.
- [35]. M. S. Omar, "Structural and Thermal Properties of Elementary and Binary Tetrahedral Semiconductor Nanoparticles," *International Journal of Thermophysics*, vol. 37, no. 1, pp. 11, 2016.
- [36]. C. C. Yang and Q. Jiang, "Temperature–pressure phase diagram of germanium determined by Clapeyron equation," *Scripta Materialia*, vol. 51, no. 11, pp. 1081-1085, 2004.